[CANCER RESEARCH 63, 2578–2584, May 15, 2003]

Tumor Classification Based on Gene Expression Profiling Shows That Uveal Melanomas with and without Monosomy 3 Represent Two Distinct Entities[1]

Frank Tschentscher, Johannes Hüsing, Tanja Hölter, Elisabeth Kruse, Irina Gana Dresen, Karl-Heinz Jöckel, Gerasimos Anastassiou, Harald Schilling, Norbert Bornfeld, Bernhard Horsthemke, Dietmar Rudolf Lohmann,[2] and Michael Zeschnigk

Institut für Humangenetik [F. T., B. H., D. R. L., M. Z.], Institut für Medizinische Informatik, Biometrie und Epidemiologie [J. H., T. H., E. K., I. G. D., K-H. J.]; and Zentrum für Augenheilkunde [G. A., H. S., N. B.], Universitätsklinikum Essen, 45122 Essen, Germany

ABSTRACT

Uveal melanoma is the most common intraocular malignancy. About 50% of patients die of metastases, which almost exclusively originate from primary tumors that have lost one chromosome 3 (monosomy 3). To gain insight into the biological mechanisms that underlie the various metastasizing potential of uveal melanoma, we have determined gene expression levels in 20 primary tumors using oligonucleotide microarrays containing 12500 probe sets. The expression measurements of those 7902 genes that were expressed in more than 10% of tumors were analyzed using two different statistical approaches. We used a modified Wilcoxon rank-sum test to identify genes differentially expressed between tumors with and without monosomy 3. Seven genes showed complete loss of expression in tumors with monosomy 3 but were expressed in tumors with disomy 3. Two of them, *CHL1* and *fls485*, are located within or close to the uveal melanoma susceptibility locus *UVM2* at 3p25. However, mutation analysis of both genes in eight tumors with monosomy 3 did not reveal structural or epigenetic alteration. To identify tumor classes, we performed unsupervised hierarchical cluster analysis; this approach separated uveal melanomas into two groups. We found that this classification is strikingly robust because, when tested by "resampling," the same grouping is obtained from 47 of 50 subsamples of genes. In clusterings of the three remaining subsamples, the grouping of only one tumor does not conform with the original classification. Excluding this tumor, cluster analyses of subsamples containing as few as 300 randomly chosen genes consistently result in the same classification, thus indicating that the difference between the two tumor classes is pervasive. Interestingly, all of the tumors in one of the groups have disomy 3, whereas all of the others have monosomy 3. Our findings suggest that there are two distinct entities of uveal melanoma that were previously unrecognized because they are not obviously distinguishable by clinicopathological features.

INTRODUCTION

Uveal melanoma is the most common intraocular malignancy (1). The incidence of this tumor increases with age and reaches a maximum between the 6th and 7th decade of life. Approximately 50% of patients die of metastases, a proportion that, despite all efforts to improve treatment, has remained constant during the last century. The average life expectancy after diagnosis of metastases is 7 months (2–4).

Cytogenetic analyses and comparative genomic hybridization have revealed recurrent chromosomal aberrations, including chromosomes 3, 6, and 8 (5, 6). Loss of an entire chromosome 3, which is an early event in tumorigenesis, is detected in ~50% of tumors (7, 8). Long-term studies have shown that ~70% of patients with monosomy 3 in the primary tumor have died of metastases within 4 years after the initial diagnosis, whereas tumors with normal chromosome 3 status (disomy 3) rarely gave rise to metastatic disease (9). Consequently, monosomy 3 is a highly specific prognostic marker for poor prognosis. The prognostic significance of parameters other than monosomy 3, *e.g.*, vascular patterns (10), cell type, tumor diameter or location, is still under discussion.

It has been proposed, that the loss of one chromosome 3 is part of a two-step mutation mechanism typical for the inactivation of tumor suppressor genes. In support of this hypothesis, we identified two regions of deletion overlap on chromosome 3 (designated *UVM1* and *UVM2*; OMIM3 606661; Ref. 11). These loci provide information on the location of putative suppressor genes in uveal melanoma. Assuming that inactivated genes show reduced transcript levels, putative suppressor genes might be detected by global expression analysis if including the positional information contributed by known regions of deletion overlap.

We have performed expression analysis in 20 uveal melanomas using oligonucleotide microarrays containing more than 12,500 probe sets. We used the data to identify genes differentially expressed between uveal melanomas with and without monosomy 3. Expression data were also used for tumor class discovery by unsupervised hierarchical cluster analysis. We applied bootstrap analysis and clusterings of small subsamples of expressed genes to test the reliability of the observed tumor classification.

MATERIALS AND METHODS

Patients and Tumor Specimens. All of the patients were given diagnosess according to current ophthalmologic criteria. Informed consent of the patients was obtained before tumor sampling. Vital tumor samples were obtained from patients treated by primary enucleation without prior radiation or chemotherapy. Tumor (snap-frozen in liquid N_2) and peripheral blood samples were obtained at the time of surgery and were stored at −80 and −20°C, respectively.

Histological Examination and Genotyping. Each tumor was classified according to cell type by conventional histology using the modified Callender system (12). Its location and degree of extension were noted. For the evaluation of vascular patterns, conventional periodic acid Schiff staining without hematoxylin counterstaining after bleaching for strong pigmented sections was performed. The vascular patterns were visible with a conventional microscope using a dark green filter and were classified according to the guidelines of Folberg *et al.* (10). DNA extraction from blood and tumor samples and microsatellite analysis, which was used for the identification of alterations of chromosomes 3, 6, and 8, were performed as described previously (13). Chromosome 6p alterations were not determined in three samples because of shortage of DNA.

Microarray Analysis. Analysis was performed on RNA derived from 20 tumors that, in microsatellite analysis of informative chromosome 3 loci, showed either complete loss of the signal of one allele (10 tumors) or no allelic imbalance (10 tumors). Total RNA was isolated from primary tumor samples using a column-based method (Qiagen RNeasy; Qiagen, Hilden, Germany). Approximately 20 μg of RNA were obtained per sample. Biotinylated "cRNA targets" were prepared according to the manufacturer's instructions (Affymetrix Expression Analysis Technical Manual; Affymetrix, Santa Clara, CA. Briefly, 6 μg of RNA were transcribed to double-stranded cDNA using the

Received 9/23/02; accepted 3/13/03.

The costs of publication of this article were defrayed in part by the payment of page charges. This article must therefore be hereby marked *advertisement* in accordance with 18 U.S.C. Section 1734 solely to indicate this fact.

[1] Supported as part of the biochip initiative by the Ministerium ("Biochip Initiative Nordrhein Westfalen") and the Deutsche Forschungsgemeinschaft (LO 530/3-3 and KFO 109/1).

[2] To whom requests for reprints should be addressed, at Universitätsklinikum Essen Hufelandstrasse 55, 45122 Essen, Germany. Phone: 49-201-723-4562; Fax: 49-201-723-5900; E-mail: dr.lohmann@uni-essen.de.

Custom SuperScript ds-cDNA Synthesis kit (Life Technologies, Inc., Karlsruhe, Germany). Included in the reaction was a T7-$(dT)_{24}$ primer containing a T7 RNA polymerase promoter site (primer sequence: 5′-GGCCAGTGAATTGTAATACGACTCACTATAGGGAGGCGG-$(dT)_{24}$-3′). cDNA was transcribed to ~60 μg of biotinylated cRNA with the BioArray HighYield RNA Transcript Labeling kit (Enzo Diagnostics, Farmingdale, NY). The cRNA samples were hybridized to HG-U95Av2 oligonucleotide arrays containing ~12,500 probe sets. Hybridization, washing, staining, and scanning was performed following standard Affymetrix protocols (Technical Manual). To enable the comparison of all of the arrays, the average intensity of all of the genes was set to 1000 before analyses. Expression values (average difference) for each gene were calculated by use of the Affymetrix Microarray Suite 4.0 analysis software. For data analysis, each probe set was considered as a separate gene.

Data Analysis. For additional statistical analyses, all of the average difference values and gene information were exported to SAS 8.2, and expression values below 50 were set to 50. For subsequent analyses, genes that were called "present" or "marginal" by the Affymetrix software in more than 10% of the tumors were included in the dataset and are referred to as "expressed genes." We used the Wilcoxon rank-sum statistic (14) as the central means to identify genes differentially expressed between tumors with monosomy 3 and disomy 3. This way, a consistently differentially expressed gene would show up regardless of its absolute expression level. To take single exceptions into account, we recalculated Wilcoxon rank sum for all of the 20 subsets in which one tumor in turn was excluded, and we maximized overall subsets. This analysis is referred to as "leave-one-out Wilcoxon" in the "Result" section. Fold change was calculated by dividing the median of the average difference values of all of the tumors with disomy 3 by the median of the average difference values of all of the tumors with monosomy 3.

Before hierarchical clustering, all of the expression values were divided by the median of a respective gene across all of the tumors, followed by log2 transformation. We applied an average linkage hierarchical clustering algorithm to group tumors according to similar expression patterns (15). Spearman rank correlation was used as a nonparametric distance function. We used bootstrapping to obtain a statistical estimate of the reliability of a grouping. We generated 50 subsamples of the same size with replacement so that any data point could be sampled multiple times or not at all (16), and we performed cluster analysis based on those subsamples. To assess how many genes were needed to find stable grouping, we performed cluster analysis with small samples generated without replacement. This process was iterated 50 times for each sample size.

Real-Time QRT-PCR. Single-stranded cDNA was generated from 1 μg of total RNA by the use of random hexamers in a 25-μl reaction using the GeneAmp RNA PCR kit [Applied Biosystems (ABI), Foster City, CA]. QRT-PCR[3] was performed in a 20-μl reaction volume containing 40 ng of cDNA, 300 nM each primer, 250 nM TaqMan probe and 1× TaqMan Universal PCR Master Mix (ABI) according to the manufacturer's instructions. Reaction was monitored in an ABI PRISM 7700 Sequence Detection System (Applied Biosystems). To amplify *CHL1* (GenBank accession no. GI-5729766), *fls485* (GenBank accession no. GI-7705707), and *HTR2B* cDNA sequences (GenBank accession no. GI-4504538) specific primers and probes were designed using the Primer Express Software (PE Applied Biosystems). Primers and TaqMan probes (see Table 1 in supplementary data)[4] were chosen to the effect that genomic DNA was not detectable. To correct for the amount of cDNA added to any individual reaction, PCR was performed in triplicate. The expression of the gene of interest was calculated relative to the β actin (*ACTB*) mRNA, which was detected with the "Pre-developed TaqMan assay β actin" (ABI). Relative expression values were calculated as described in the "User Bulletin no. 2: ABI PRISM 7700 Sequence Detection System."

Sequence Analysis. All of the coding of the exons of the *CHL1* (exons 3–28) and *fls485* (exons 1–12) were PCR amplified and sequenced directly by the use of a standard cycle sequencing protocol provided by the manufacturer on an ABI automated sequencer (ABI PRISM 3100 Genetic Analyzer). Primers (see supplemental material)[4] that were used for amplification and sequence analysis were derived from published sequences (NCBI Accession: NT_005927).

MSP. Bisulfite treatment of 5 μg of tumor DNA was performed as described elsewhere (17). PCR was performed in a 25-μl reaction volume containing 2 μl of bisulfite-treated DNA, 10 mM Tris-HCl (pH 8.3), 50 mM KCl, 1.5 mM $MgCl_2$, 200 μM each dNTP, 1 unit AmpliTaq (Applied Biosystems), and 1 μM each primer (CHL1met5′ and CHL1met3′ for the amplification of the methylated allele and CHLunmet5′ and CHLunmet3′ for the amplification of the unmethylated allele, respectively). After initial denaturation at 95°C for 2 min, 35 cycles (denaturation at 95°C for 15 s, annealing at 64°C for 15 s and extension at 72°C for 30 s, were performed, followed by a final extension at 72°C for 5 min. MSP products were separated by electrophoresis on 2% agarose gels and were visualized by ethidium bromide staining. The MSP was controlled by the use of methylated control DNA as a template. Primer sequences were as follows: CHLmet3′: 5′-CACGAAAAACCCC-CCCAACGCCGACACG-3′; CHLmet5′: 5′-CGGGA GGGGACGGGCGG-GATTTTCGC-3′; CHLunmet3′: 5′-CACAAAAAACCCCCCCAACA CCA-ACACA-3′; CHLunmet5′: 5′-TGGGAGGGGATGGGTGGGATTTTTGT-3′.

Competitive PCR. Assays were developed to identify possible homozygous deletions of *CHL1* or *fls485*. For each gene, two duplex PCRs were established, each containing primers to amplify a transcribed region and for a control region on chromosome 3 (*fls485* exon1 (30 μM) + D3S2386 (100 μM); *fls485* exon 11 (5 μM) + WI936 (100 μM); *CHL1* exon27 (100 μM) + GATA87B02 (50 μM); *CHL1* exon3 (100 μM) + WI1780 (20 μM)). For primer sequences see supplementary material[4] and public database UniSTS of the National Center for Biotechnology Information, Bethesda, Maryland.[5] PCR was performed in a final volume of 25 μl containing 10 mM Tris-HCl (pH 8.3), 50 mM KCl, 1.5 mM $MgCl_2$, 1 unit AmpliTaq (Applied Biosystems), 50 μM each dNTP, and 50 ng of tumor or blood DNA (primer concentration see above). After initial denaturation at 95°C for 2 min, 35 cycles of amplification were performed as follows: 15 s at 95°C, 15 s at 58°C, and 30 s at 72°C, followed by 72°C for 10 min. PCR products were analyzed on 2% agarose gels followed by ethidium bromide staining. The intensity of bands was inspected visually.

Supplementary Data and Material. Ancillary data including primary expression data and primer sequences can be obtained online.[4]

RESULTS

We analyzed the expression patterns of ~12,500 genes in 20 primary uveal melanomas by hybridizing labeled cRNA samples onto oligonucleotide microarrays (for all average difference values see Table 3, supplementary data).[4] The average difference values of 7902 genes, which were found to be expressed in more than 10% of the tumors (Table 4, supplementary data),[4] were analyzed by two different statistical methods.

To identify genes differentially expressed between uveal melanomas with disomy 3 and monosomy 3, we applied the Wilcoxon rank-sum test using the chromosome 3 status of a tumor as the preset parameter. We identified 36 genes with the lowest possible rank sum of 55. These genes show lower expression in all tumors with monosomy 3 compared with tumors with disomy 3. The highest possible rank sum of 155 was found for six genes that are expressed at higher levels in all tumors with monosomy 3. To account for possible biological variability, we also performed a "leave-one-out Wilcoxon" analysis. This approach, which permits one tumor in turn to be in exception to the perfect separation, identified an additional 119 and 38 genes with the lowest and the highest possible rank sum, respectively.

For each of the 201 genes identified by Wilcoxon analysis, we determined the fold change (Table 2, supplementary data).[4] Fig. 1 lists all of the 34 genes (2 genes are represented by two probe sets) with a fold change of at least 3 and all of the 8 genes with transcripts absent in at least 9 of 10 tumors in one of either group. Seven of the eight genes showed loss of expression in tumors with monosomy 3. Interestingly, two of these genes, *CHL1* and *fls485*, map within or close to

[3] The abbreviations used are: QRT-PCR, (real-time) quantitative reverse transcription-PCR; MSP, methylation-specific PCR; MMP, matrix metalloproteinase; TIMP, tissue inhibitor of MMP; GO, gene ontology; OMIM, Online Mendelion Inheritance in Man.

[4] Internet address: http://www.uni-essen.de/humangenetik/download.

[5] Internet address: http://www.ncbi.nlm.nih.gov/genome/sts.

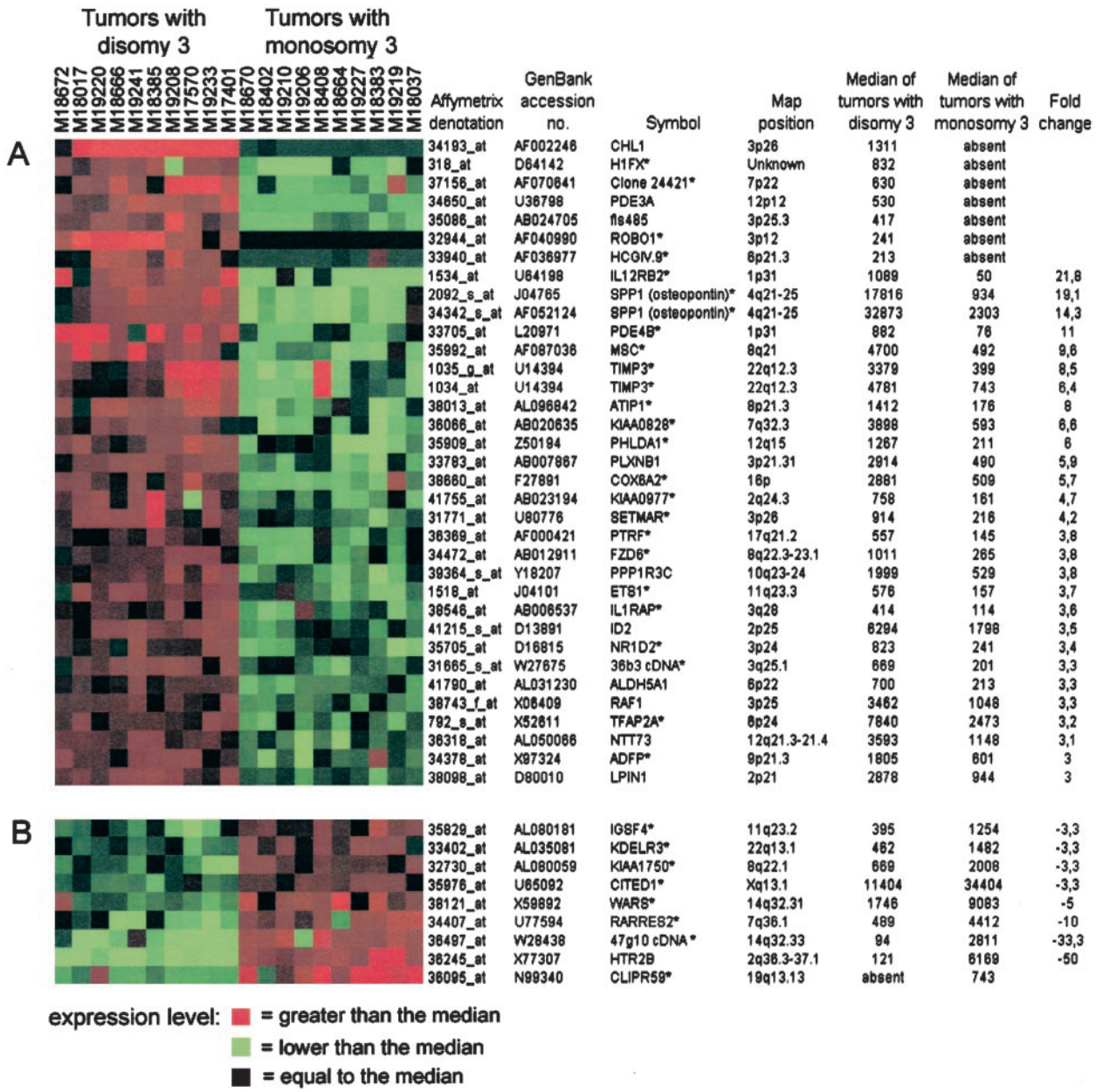

	Affymetrix denotation	GenBank accession no.	Symbol	Map position	Median of tumors with disomy 3	Median of tumors with monosomy 3	Fold change
A	34193_at	AF002246	CHL1	3p26	1311	absent	
	318_at	D64142	H1FX*	Unknown	832	absent	
	37156_at	AF070641	Clone 24421*	7p22	630	absent	
	34650_at	U36798	PDE3A	12p12	530	absent	
	35086_at	AB024705	fls485	3p25.3	417	absent	
	32944_at	AF040990	ROBO1*	3p12	241	absent	
	33940_at	AF036977	HCGIV.9*	6p21.3	213	absent	
	1534_at	U64198	IL12RB2*	1p31	1089	50	21,8
	2092_s_at	J04765	SPP1 (osteopontin)*	4q21-25	17816	934	19,1
	34342_s_at	AF052124	SPP1 (osteopontin)*	4q21-25	32873	2303	14,3
	33705_at	L20971	PDE4B*	1p31	882	76	11
	35992_at	AF087036	MSC*	8q21	4700	492	9,6
	1035_g_at	U14394	TIMP3*	22q12.3	3379	399	8,5
	1034_at	U14394	TIMP3*	22q12.3	4781	743	6,4
	38013_at	AL096842	ATIP1*	8p21.3	1412	176	8
	36066_at	AB020635	KIAA0828*	7q32.3	3898	593	6,6
	35909_at	Z50194	PHLDA1*	12q15	1267	211	6
	33783_at	AB007867	PLXNB1	3p21.31	2914	490	5,9
	38660_at	F27891	COX6A2*	16p	2881	509	5,7
	41755_at	AB023194	KIAA0977*	2q24.3	758	161	4,7
	31771_at	U80776	SETMAR*	3p26	914	216	4,2
	36369_at	AF000421	PTRF*	17q21.2	557	145	3,8
	34472_at	AB012911	FZD6*	8q22.3-23.1	1011	265	3,8
	39364_s_at	Y18207	PPP1R3C	10q23-24	1999	529	3,8
	1518_at	J04101	ETS1*	11q23.3	576	157	3,7
	38546_at	AB006537	IL1RAP*	3q28	414	114	3,6
	41215_s_at	D13891	ID2	2p25	6294	1798	3,5
	35705_at	D16815	NR1D2*	3p24	823	241	3,4
	31665_s_at	W27675	36b3 cDNA*	3q25.1	669	201	3,3
	41790_at	AL031230	ALDH5A1	6p22	700	213	3,3
	38743_f_at	X06409	RAF1	3p25	3462	1048	3,3
	792_s_at	X52611	TFAP2A*	6p24	7840	2473	3,2
	36318_at	AL050066	NTT73	12q21.3-21.4	3593	1148	3,1
	34378_at	X97324	ADFP*	9p21.3	1805	601	3
	38098_at	D80010	LPIN1	2p21	2878	944	3
B	35829_at	AL080181	IGSF4*	11q23.2	395	1254	-3,3
	33402_at	AL035081	KDELR3*	22q13.1	462	1482	-3,3
	32730_at	AL080059	KIAA1750*	8q22.1	669	2008	-3,3
	35976_at	U65092	CITED1*	Xq13.1	11404	34404	-3,3
	38121_at	X59892	WARS*	14q32.31	1746	9083	-5
	34407_at	U77594	RARRES2*	7q36.1	489	4412	-10
	36497_at	W28438	47g10 cDNA*	14q32.33	94	2811	-33,3
	36245_at	X77307	HTR2B	2q36.3-37.1	121	6169	-50
	36095_at	N99340	CLIPR59*	19q13.13	absent	743	

Fig. 1. Color mosaic plot and table with expression levels and map positions of the 42 genes with the lowest and highest possible rank-sum value and with a fold change greater than 3 or loss of expression in one of either group. ∗, genes identified by the "leave-one-out Wilcoxon" analysis. A gene is referred to as absent if it was called "absent" in at least 9 of 10 tumors in one of either group by the Affymetrix software. The median-polished normalized ratio of gene expression in an individual tumor is indicated by the color of each square. The color saturation indicates the degree of difference from the median. *A*, genes with lower expression in tumors with monosomy 3. *B*, genes with lower expression in tumors with disomy 3.

the uveal melanoma susceptibility locus *UVM2* at 3p25. We used an insertion/deletion polymorphism in intron 7 of *fls485* and single nucleotide polymorphisms in exons 3, 9, and 13 of the *CHL1* gene, to detect allele losses of both genes in tumors that define the *UVM2* region at 3p25 (tumors M13789 and M16397 (see Ref. 11). We found loss of heterozygosity for the intronic *fls485* polymorphism in both tumors thus proving that this gene is located within this region (data not shown). Heterozygosity of polymorphic sites within *CHL1* was lost in tumor M16397 but was retained in tumor M13789, thus indicating that *CHL1* is located outside *UVM2*.

To assess the transcript levels of *CHL1* and *fls485* by an independent method, we performed QRT-PCR in 10 tumors randomly chosen from the series used for microarray analysis. The serotonin receptor *HTR2B*, which is one of the six differentially expressed genes with a rank sum of 155, was included in QRT-PCR analyses. As shown in Fig. 2*a*, the average difference values as determined by microarray analysis were in agreement with the relative transcript quantities as measured by QRT-PCR. To analyze whether differentially expression of *CHL1*, *fls485*, and *HTR2B* is replicated in another set of tumors, we performed QRT-PCR analysis on an additional 20 uveal melanomas: 11 tumors with monosomy 3 and 9 tumors with disomy 3. In 17 of 20 tumors. the relative expression levels of *CHL1*, *fls485*, and *HTR2B* correspond to the findings in the set of tumors analyzed by microarray hybridization. In tumors M18410 and M17373 with monosomy 3, the expression of *HTR2B* was rather low. The latter tumor also showed clearly detectable transcript levels of *CHL1* and *fls485*. In tumor M18025 with disomy 3, the expression levels of *CHL1*, *fls485*, and *HTR2B* conformed with the pattern typical for tumors with monosomy 3 (Fig. 2*b*).

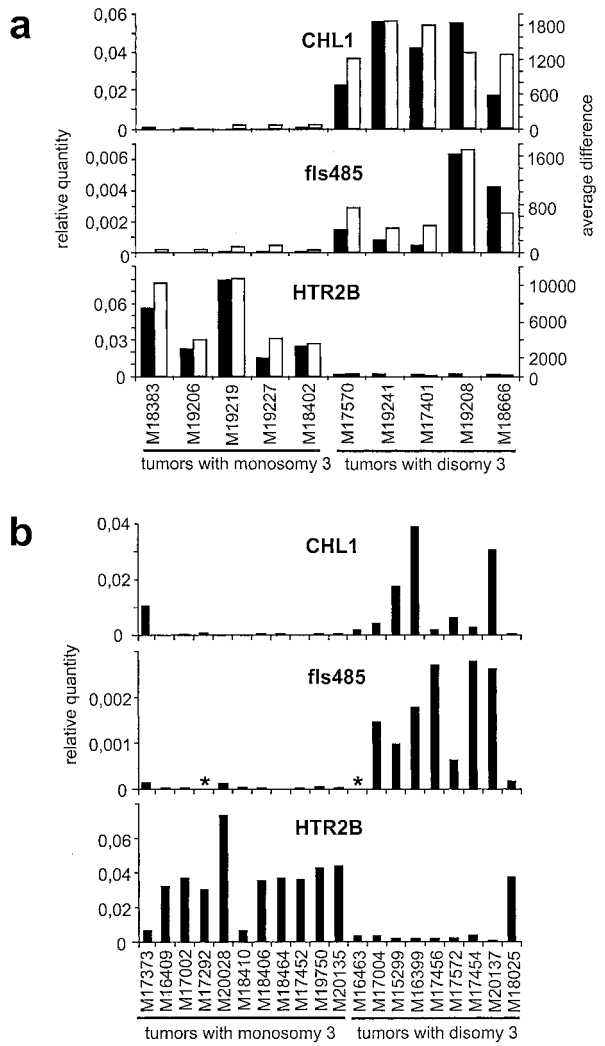

Fig. 2. QRT-PCR analysis of *fls485*, *HTR2B*, and *CHL1*. The mean of the results obtained by triplicate PCR assays is shown. The mRNA expression level of each gene is given relative to the β actin (*ACTB*) mRNA level. *a*, comparison of expression levels obtained by QRT-PCR (*black bars*) and microarray analysis (*open bars*) in 10 tumors randomly chosen from the set used for microarray analysis. *b*, QRT-PCR analysis of *fls485*, *HTR2B*, and *CHL1* in another panel of 20 tumors. ∗, PCR failure.

Because microarray and QRT-PCR results showed an absence of *CHL1* and *fls485* transcripts in almost all of the tumors with monosomy 3, we searched for mutations that might account for this. We identified no homozygous deletion in *CHL1* and *fls485* in 45 and 36 tumors with monosomy 3, respectively. Sequence analysis of all of the coding exons of *CHL1* and *fls485* in eight tumors with monosomy 3 showed polymorphic variants but no mutation. We also investigated methylation of the *CHL1* gene promoter by MSP. We detected no methylated allele in any of the 5 tumors with disomy 3 or 12 tumors with monosomy 3 that were tested (data not shown). Because there is no CpG island in the 5′ region of the *fls485* gene, transcriptional inactivation by promoter methylation is unlikely for this gene (18).

Next, we used the data set of the 7902 expressed genes for unsupervised hierarchical cluster analysis using Spearman rank correlation as similarity measure (15). This algorithm allows the separation of tumor samples into groups based on the similarity of their gene expression patterns without prior knowledge of sample identity. In the resulting tree, two discrete clusters were formed (Fig. 3*a*). We tested whether the two groups identified by this classification are associated with clinicopathological features or genetic alteration. Interestingly, all nine of the tumors in one of the two clusters showed disomy 3, whereas in the other group, all but one tumor had monosomy 3 ($P < 0.0001$, Fisher's exact test). The two tumor classes showed no significant association with any other clinicopathological features or genetic alteration (Fig. 3*a*). Specifically, neither vascular patterns nor tumor diameter (data not shown) are specific features of either of the clusters (*P*s greater than 5%). Only chromosome 8q alterations ($P = 0.065$) and ciliary body involvement ($P = 0.07$) came close to statistical significance.

To assess whether the observed tumor classification is a simple consequence of reduced dosage of chromosome 3 genes in tumors having one chromosome 3 only, we excluded those 251 expressed genes from the dataset that were found to be located on chromosome 3 (see supplementary data).[4] Cluster analysis of the expression data of the remaining 7651 genes generated the same two distinct clusters of tumors (Fig. 3*b*). To assess the robustness of the observed clustering results, we applied bootstrapping on the original dataset of 7902 and on the dataset without chromosome 3 gene (19). From each dataset, we generated 50 bootstrap samples and performed cluster analysis. For both datasets, 47 of 50 bootstrap samples resulted in the same two distinct clusters of tumors (Fig. 3, *a* and *b*). In each of the 3 various samples only one tumor, M18672, did not maintain class assignment.

We also performed cluster analysis with subsamples of randomly chosen genes. We excluded tumor M18672 from this analysis, because class assignment of this tumor was found to be unstable in bootstrap analysis. All 50 subsamples containing 2000 genes resulted in the original classification that was obtained with all 7902 genes. When decreasing the size of the random subsamples, this classification remained predominant even when clustering as few as 300 genes (Fig. 4).

We also tested whether the expression profiles of functionally related genes contribute more or less to the dissimilarity of the two tumor classes. We used the assignment of genes to functionally related groups as provided by the GO consortium (20). We compared the

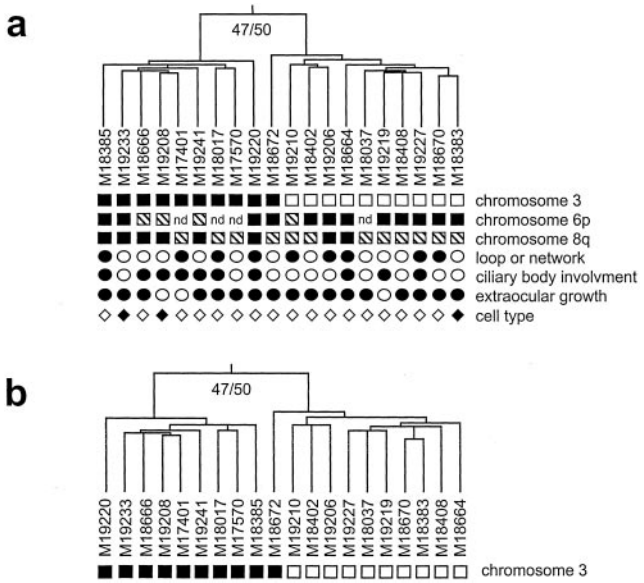

Fig. 3. Tumor classification as obtained by hierarchical cluster analysis of the expression data for 20 uveal melanomas. The proportion of bootstrap analyses that replicate the same two classes of tumors is shown at the top of each tree. *a*, cluster analysis based on the expression data of 7902 expressed genes. *Below the name of each tumor* (*across the top*), the genetic, clinical and histopathological characteristics are indicated by symbols: *filled/open/hatched boxes*, retention of alleles/loss of heterozygosity/allelic imbalance; *filled/open circles*, no/yes as to ciliary body involovemnt and extraocular growth; *filled/open diamonds*, spindle/mixed cell type. *nd*, not determined because of shortage of DNA. *b*, cluster analysis based on the expression data of a subset of 7651 expressed genes excluding genes found to be located on chromosome 3.

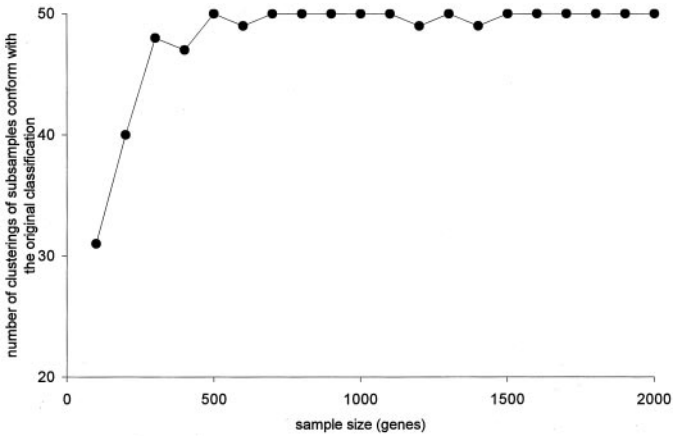

Fig. 4. Clustering of subsamples of randomly chosen genes. Sample sizes ranging from 100 to 2000 genes at intervals of 100 were used. For each sample size, cluster analyses was iterated 50 times. The number of cluster analyses that result in the original classification obtained with all 7902 genes is shown for each sample size. Analysis is based on the expression data of 19 tumors excluding tumor M18672.

distribution of Wilcoxon rank sums of subsamples containing functionally related genes that were identified by the following GO terms: protein kinase (GO:4672); RNA polymerase II transcription factor (GO:3702); carbohydrate metabolism, (GO:5975); DNA repair (GO:6281); lipid metabolism (GO:6629); oncogenesis (GO:7048); cell adhesion (GO:7155); cell surface receptor-linked signal transduction (GO:7166); protein biosynthesis (GO:6412); and structural molecule (GO:5198). All but one of these subsamples showed a distribution of Wilcoxon rank sums similar to the one obtained with the dataset containing all of the expressed genes (data not shown). This indicates that the expression patterns of genes assigned to diverse biological pathways contribute to the clustering of the two tumor groups. A distinct distribution of Wilcoxon rank sums is seen only for the subset containing 98 genes involved in protein biosynthesis (GO:6412; Fig. 5). When breaking down the components of this subset we found that the observed deviation is mainly based on the two bins on the left site of the histogram that comprise 55 genes with Wilcoxon rank sums ranging from 55 to 74. These 55 genes showed a fold change that ranged from 1.2 to 2.4 (supplementary data).[4] Most of them code for cytoplasmic ribosomal proteins, whereas the remaining genes of this group GO:6412, mostly aminoacyl-tRNA-synthetases, show no differential expression. This suggests that genes for cytoplasmic ribosomal proteins are coregulated. A similar observation was reported in tumor and normal colon tissue (21), thus indicating that these changes are not specific for uveal melanomas.

DISCUSSION

Metastasizing uveal melanoma originates almost exclusively from primary tumors that have lost one chromosome 3 early in tumorigenesis (7, 9), thus suggesting that one or more metastasis suppressor genes are located on chromosome 3. Actually, of all 7 genes that were absent in tumors with monosomy 3 but that were expressed in tumors with disomy 3, three are located on chromosome 3. Two of these genes, *CHL1* and *fls485*, are candidate suppressor genes because they are mapped within or close to the uveal melanoma susceptibility locus *UVM2* at 3p25, which was previously identified as smallest region of deletion overlap (11). Interestingly, a lower expression of *CHL1* was also found in a highly invasive uveal melanoma cell line when compared with a poorly invasive line that was derived from the same metastatic lesion (22). *CHL1* is a member of the *L1CAM* gene family, which encodes neural cell adhesion molecules required for migration and differentiation of neuronal cells. The function of the *fls485* gene, which was identified in a cDNA library prepared from fetal liver mRNA, is not elucidated yet. We cannot exclude that, despite drastically reduced transcript levels, there is still enough protein for normal function. Typically, loss of expression of tumor suppressor genes is a consequence of allele loss and mutations or epigenetic alterations in the remaining allele but we did not identify any structural or epigenetic alterations in *CHL1* and *fls485* in DNA from 8 tumors with monosomy 3 that could account for the absence of their transcripts. However, recent data indicate that inactivation of suppressor genes in tumors can also result from other mechanisms. In metastatic cutaneous melanoma, tumors with allele loss in the region of the *Apaf-1* gene also show loss of expression of *Apaf-1*, although no structural alteration or promoter methylation was identified in the remaining allele (23). Interestingly, in cell lines derived from these tumors, expression of *Apaf-1* was restored after incubation with 5-aza-2′-deoxycytidine, a nucleotide analogue that cannot be methylated, thus indicating that transcriptional silencing depends on methylation of DNA outside the promoter region of this gene. This shows that inactivation of suppressor genes is not necessarily dependent on mutations or epigenetic alterations within the gene and points to the possible role of distant *cis*-regulatory elements.

Several genes show highly significant differential expression between tumors with and without monosomy 3 (Fig. 1) and some of them have been implicated in progression of tumors other than uveal melanoma. One of these genes is osteopontin (*SPP1*), which codes for a cytokine that can bind to several integrins and various isoforms of CD44 and can also function as a cell adhesion protein. In various cancers, expression of osteopontin was found to be a marker for metastatic disease (for review see 24, 25). Recently, gene expression profiling in colon cancers of multiple stages has shown that osteopontin expression is correlated with advanced tumor stages (26). In uveal melanoma, however, high transcript levels of osteopontin were only present in tumors with disomy 3, which rarely give rise to metastatic disease. This indicates that high levels of osteopontin are not a marker for metastatic disease in all tumor types. Another differentially expressed gene is *TIMP-3*. Tissue inhibitors of metalloproteinases (TIMPs) negatively regulate the activity of MMPs, which are important for remodeling of the extracellular matrix (27). In several tumors, increased activity of MMPs has been associated with malignant progression (for review see 28). Although, recent data indicate that the role of TIMPs is more complex and that some TIMPs may also promote tumorigenesis by growth stimulatory and antiapoptotic ef-

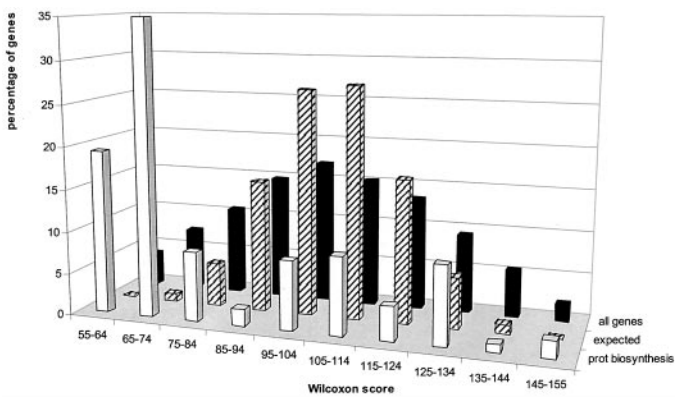

Fig. 5. The distribution of Wilcoxon rank sums of all (7902) expressed genes (*black bars*) and 98 genes involved in protein biosynthesis (*open bars*). *Hatched bars*, distribution of Wilcoxon rank sums as expected under the assumption of independence between gene expression profiles and tumor classification (theoretical null distribution). *The bar height*, the percentage of genes with the indicated Wilcoxon rank sums. *Each bar*, a bin width of 10.

fects (28), no such activities have been reported for *TIMP-3* thus far. Therefore, low to absent expression of *TIMP-3*, as observed in 9 of 10 uveal melanomas with chromosome 3 loss, might significantly contribute to the high metastatic potential of these tumors. Whereas osteopontin and TIMPs were found to be involved in the progression toward metastatic disease (25), no such role has been reported for *HTR2B* thus far. We found high transcript levels of this gene in all uveal melanomas with monosomy 3 compared with low expression in all tumors with disomy 3. As monosomy 3 is associated with metastatic disease, *HTR2B* might serve as a marker to identify patients with poor prognosis. This might be done by using immune histochemistry analysis on primary tumor samples, a methodology that is straightforward compared with cytogenetic or molecular evaluation of chromosome 3 loss. Moreover, expression of this proposed marker may be used to detect disseminated tumor cells in blood or other readily accessible biological samples. This would permit prognostic stratification in many patients from whom, because of conservative therapy, no tumor material is available.

Unsupervised hierarchical cluster analysis of the expression data separated the 20 uveal melanomas into two groups. The two classes of tumors identified by these clusters are, barring one tumor, completely associated with the status of chromosome 3. However, this classification is not a simple consequence of gene dosage-related expression changes, because the structure of the tree is essentially unchanged after exclusion of expression data of genes known to be located on chromosome 3. The classification is also robust because clusterings of 47 of 50 bootstrap samples resulted in the same two distinct classes of tumors. In the three discordant bootstrap trees, only one tumor does not maintain class assignment. Interestingly, this is also the tumor not classified consistent with its chromosome 3 status. Possibly, this tumor would become part of a third, smaller-sized cluster, if expression data from a substantially larger set of tumors were available. If excluding this tumor, the majority of clusterings obtained from random representations containing as few as 300 genes establish the same classification as obtained with all 7902 of the expressed genes. This shows that the expression patterns of a large proportion of genes contribute to the classification and indicates a high degree of molecular dissimilarity between the tumors assigned to these classes. In a further analysis we compared Wilcoxon rank-sum distributions of subsets of functionally related genes to identify whether some subsets contribute more or less to the dissimilarity between tumor classes. Only the subset of genes involved in protein synthesis showed a clearly distinct distribution, which was characterized by coordinate down-regulation of genes for ribosomal proteins but not of aminoacyl-tRNA-synthetases in tumors with monosomy 3. This suggests that the expression of these functionally related components of the translation machinery is unbalanced in uveal melanomas with monosomy 3. It remains to be tested whether or not this finding is correlated with the variation of nucleolus size that has been found to be a prognostic marker in uveal melanoma (12, 29). The distribution of Wilcoxon rank sums of the other nine subsets of functionally related genes is almost identical to that obtained with all 7902 expressed genes. This indicates that the dissimilarity between the two classes of uveal melanomas is based on the expression patterns of genes assigned to diverse biological pathways.

The two classes of uveal melanoma identified by unsupervised cluster analysis are distinguished by a pervasive difference in their gene expression patterns and, therefore, may be regarded as two distinct tumor entities. Alterations of chromosome 8 and 6 are found in tumors of both classes, and, therefore, the two presumed entities possibly share some molecular mechanisms of transformation. However, monosomy 3, which is an early event in the development of uveal melanoma, is confined to only one of these classes. Consequently, the dissimilarity of gene expression patterns might result from distinct initiation pathways of tumors with or without chromosome 3 loss. Alternatively, a dissimilar gene expression pattern could also result if the two entities originate from different cells. Uveal melanoma arises from melanocytes in the uveal tract, which, like their cutaneous counterparts, are derived from the neural crest. Despite the common embryonal origin of their precursor cells, clinical behavior and molecular biology of uveal and cutaneous melanoma are distinct, thus indicating the influence of the tissue from which the tumors have originated. However, the uveal tract is not a uniform tissue but is composed of morphologically and functionally distinct parts including the iris, ciliary body, and choroid. Therefore, it is not unreasonable to assume that uveal tissues are populated by different melanocytes that give rise to melanomas with distinct expression profiles. This hypothesis would also account for the variation of chromosome 3 status between tumors located in the ciliar and posterior part of the eye, which is also present in our data (30).

In the present study, we have investigated tumors from patients with recent diagnoses of uveal melanoma, and, therefore, data on metastasis formation are not yet available. However, it is well established that uveal melanomas with disomy 3 rarely give rise to metastatic disease (9). This suggests that the genetic program of tumors with disomy 3 is unlikely to acquire the genetic changes required for metastasis formation. This corresponds to our classification data, because numerous mutations may be required to reprogram these tumors and obtain the widely different gene expression pattern observed in uveal melanomas with monosomy 3. It will be interesting to learn of the fate of the patient whose tumor, M18672, showed no loss of chromosome 3 but was grouped with monosomy 3 tumors in cluster analysis.

ACKNOWLEDGMENTS

We thank Bianca Beyer for technical assistance. We also thank Karl Worm for assistance with real-time PCR experiments and Knud Nierhaus for helpful discussion.

REFERENCES

1. Egan, K. M., Seddon, J. M., Glynn, R. J., Gragoudas, E. S., and Albert, D. M. Epidemiologic aspects of uveal melanoma. Surv. Ophthalmol., *32:* 239–251, 1988.
2. Gamel, J. W., McLean, I. W., and McCurdy, J. B. Biologic distinctions between cure and time to death in 2892 patients with intraocular melanoma. Cancer (Phila.), *71:* 2299–2305, 1993.
3. Luyten, G. P., Mooy, C. M., Eijkenboom, W. M., Stijnen, T., Hellemons, L. P., Luider, T. M., and de Jong, P. T. No demonstrated effect of pre-enucleation irradiation on survival of patients with uveal melanoma. Am. J. Ophthalmol., *119:* 786–791, 1995.
4. Lorigan, J., Wallace, S., and Mavligit, G. The prevalence and location of metastases from ocular melanoma: imaging study in 110 patients. Am. J. Roentgenol., *157:* 1279–1281, 1991.
5. Prescher, G., Bornfeld, N., and Becher, R. Nonrandom chromosomal abnormalities in primary uveal melanoma. J. Natl. Cancer Inst. (Bethesda), *82:* 1765–1769, 1990.
6. Sisley, K., Rennie, I. G., Cottam, D. W., Potter, A. M., Potter, C. W., and Rees, R. C. Cytogenetic findings in six posterior uveal melanomas: involvement of chromosomes 3, 6 and 8. Genes Chromosomes Cancer, *2:* 205–209, 1990.
7. Prescher, G., Bornfeld, N., and Becher, R. Two subclones in a case of uveal melanoma. Relevance of monosomy 3 and multiplication of chromosome 8q. Cancer Genet. Cytogenet., *77:* 144–146, 1994.
8. Wiltshire, R. N., Elner, V. M., Dennis, T., Vine, A. K., and Trent, J. M. Cytogenetic analysis of posterior uveal melanoma. Cancer Genet. Cytogenet., *66:* 47–53, 1993.
9. Prescher, G., Bornfeld, N., Hirche, H., Horsthemke, B., Jöckel, K. H., and Becher, R. Prognostic implications of monosomy 3 in uveal melanoma. Lancet, *347:* 1222–1225, 1996.
10. Folberg, R., Rummelt, V., Parys-Van Ginderdeuren, R., Hwang, T., Woolson, R. F., Pe'er, J., and Gruman, L. M. The prognostic value of tumor blood vessel morphology in primary uveal melanoma. Ophthalmology, *100:* 1389–1398, 1993.
11. Tschentscher, F., Prescher, G., Horsman, D. E., White, V. A., Rieder, H., Anastassiou, G., Schilling, H., Bornfeld, N., Bartz-Schmidt, K. U., Horsthemke, B., Lohmann, D. R., and Zeschnigk, M. Partial deletions of the long and short arm of chromosome 3 point to two tumor suppressor genes in uveal melanoma. Cancer Res., *61:* 3439–3442, 2001.

12. McLean, I. W., Foster, W. D., Zimmerman, L. E., and Gamel, J. W. Modifications of Callender's classification of uveal melanoma at the armed forces institute of pathology. Am. J. Ophthalmol., *96:* 502–509, 1983.
13. Tschentscher, F., Prescher, G., Zeschnigk, M., Horsthemke, B., and Lohmann, D. R. Identification of chromosomes 3, 6, and 8 aberrations in uveal melanoma by microsatellite analysis in comparison to comparative genomic hybridization. Cancer Genet. Cytogenet., *122:* 13–17, 2000.
14. Hollander, M., and Wolfe, D. A. Nonparametric Statistical Methods pp. 67–82. New York: John Wiley & Sons, 1973.
15. Eisen, M. B., Spellmann, P. T., Brown, P. O., and Botstein, D. Cluster analysis and display of genome-wide expression patterns. Proc. Natl. Acad. Sci. USA, *95:* 14863–14868, 1998.
16. Efron, B., and Tibshirani, R. J. An introduction to the bootstrap. New York: Chapman and Hall, 1993.
17. Zeschnigk, M., Schmitz, B., Dittrich, B., Buiting, K., Horsthemke, B., and Doerfler, W. Imprinted segments in the human genome: different DNA methylation patterns in the Prader-Willi/Angelman syndrome region as determined by the genomic sequencing method. Hum. Mol. Genet., *6:* 387–395, 1997.
18. Baylin, S. B., Esteller, M., Rountree, M. R., Bachman, K. E., Schuebel, K., and Herman, J. G. Aberrant patterns of DNA methylation, chromatin formation and gene expression in cancer. Hum. Mol. Genet., *10:* 687–692, 2001.
19. Kerr, M. K., and Churchill, G. A. Bootstrapping cluster analysis: assessing the reliability of conclusions from microarray experiments. Proc. Natl. Acad. Sci. USA, *98:* 8961–8965, 2001.
20. The Gene Ontology Consortium. Gene ontology: tool for the unification of biology. Nat. Genet., *25*: 25–29, 2000.
21. Alon, U., Barkai, N., Notterman, D. A., Gish, K., Ybarra, S., Mack, D., and Levine, A. J. Broad patterns of gene expression revealed by clustering analysis of tumor and normal colon tissues probed by oligonucleotide arrays. Proc. Natl. Acad. Sci. USA, *96:* 6745–6750, 1999.
22. Seftor, E. A., Meltzer, P. S., Kirschmann, D. A., Pe'er, J., Maniotis, A. J., Trent, J. M., Folberg, R., and Hendrix, M. J. Molecular determinants of human uveal melanoma invasion and metastasis. Clin. Exp. Metastasis, *19:* 233–246, 2002.
23. Soengas, M. S., Capodieci, P., Polsky, D., Mora, J., Esteller, M., Opitz-Araya, X., McCombie, R., Herman, J. G., Gerald, W. L., Lazebnik, Y. A., Cordon-Cardo, C., and Lowe, S. W. Inactivation of the apoptosis effector Apaf-1 in malignant melanoma. Nature (Lond.), *409:* 207–211, 2001.
24. Weber, G. F. The metastasis gene *osteopontin*: a candidate target for cancer therapy. Biochim. Biophys. Acta, *1552:* 61–85, 2001.
25. Weber, G. F., and Ashkar, S. Stress response genes: the genes that make cancer metastasize. J. Mol. Med., *78:* 404–408, 2000.
26. Agrawal, D., Chen, T., Irby, R., Quackenbush, J., Chambers, A. F., Szabo, M., Cantor, A., Coppola, D., and Yeatman, T. J. Osteopontin identified as lead marker of colon cancer progression, using pooled sample expression profiling. J. Natl. Cancer Inst. (Bethesda), *94:* 513–521, 2002.
27. Nagase, H., and Woessner, J. F., Jr. MMPs. J. Biol. Chem., *274:* 21491–21494, 1999.
28. Jiang, Y., Goldberg, I. D., and Shi, Y. E. Complex roles of tissue inhibitors of metalloproteinases in cancer. Oncogene, *21:* 2245–2252, 2002.
29. Gamel, J. W., and McLean, I. W. Quantitative analysis of the Callender classification of uveal melanoma cells. Arch. Ophthalmol., *95:* 686–691, 1977.
30. Prescher, G., Bornfeld, N., Horsthemke, B., and Becher, R. Chromosomal aberrations defining uveal melanoma of poor prognosis. Lancet, *339:* 691–692, 1992.

Tumor Classification Based on Gene Expression Profiling Shows That Uveal Melanomas with and without Monosomy 3 Represent Two Distinct Entities

Frank Tschentscher, Johannes Hüsing, Tanja Hölter, et al.

Cancer Res 2003;63:2578-2584.